Nylon 6/Organoclay Nanocomposites by Extrusion

Teresa Varela González,[1] Carlos Guerrero Salazar,[1] Javier Rivera De la Rosa,[2] Virgilio González González[1]

[1]*División de Estudios de Postgrado, Facultad de Ingeniería Mecánica y Eléctrica, San Nicolás delos Garza, N.L. 66450, Mexico*
[2]*Carrera de Ingeniería Química, Facultad de Ciencias Quimicas/Universidad Autónoma de Nuero León Torre de la Rectoría, 7° Piso, cd. Universitoria, San Nicolás de los Garza, N. L. 66450, Mexico*

Received 17 November 2006; accepted 3 June 2007
DOI 10.1002/app.27307
Published online 27 February 2008 in Wiley InterScience (www.interscience.wiley.com).

ABSTRACT: Montmorillonite-layered silicates were modified with one tertiary alkylammonium salt (ALAS), to obtain nylon 6/montmorillonite nanocomposites. Nanocomposites were prepared by direct polymer melt-intercalation, using two kinds of devices: twin-screw extruder and a Brabender Plasticorder. Composites were made with different load clay to see the effect of them in the nylon composites. The modified clay was characterized by X-ray diffraction (XRD), thermogravimetric analysis (TGA), and liquid nitrogen sorption; to evidence the intercalation of the ALAS among the layers of the montmorillonite. The nanocomposites were characterized by XRD, Fourier transform infrared spectroscopy, TGA, capillary rheometry, and mechanical tensile testing. The organoclay was well dispersed into the nylon 6 matrix when compounded with the twin-screw extruder, but the use of a Brabender Plasticorder was less effective. The mechanical properties were modified, and the tensile modulus showed a relevant change compared with the pristine nylon 6. © 2008 Wiley Periodicals, Inc. J Appl Polym Sci 108: 2923–2933, 2008

Key words: montmorillonite; alkylammonium salt; organoclay; nanocomposite

INTRODUCTION

Layered silicates dispersed in an engineering polymer matrix are one of the most important hybrid nanocomposites, because of their unique intercalation/exfoliation characteristics, high-aspect ratio, and high-interchange ionic capacity.[1,2] The efficiency of the clay as a reinforcing agent that helps to modify the physicochemical properties of the polymer is determined by the degree of its dispersion in the polymer matrix, especially when the layers are exfoliated. This is observed when polymer matrix and layered silicates have strong attraction interactions.[3] Polymer-layered silicate nanocomposites have shown some considerable property improvements over ordinary polymers; examples of improvements are the increase in strength, modulus, thermal resistance, heat distortion temperature, solvent resistance, and flame retardant capability.[4–6] However, the interactions of the components are affected by the incompatibility between them, due to the fact that layered silicates are hydrophilic and polymers have a hydrophobic character. To achieve a better interaction with the polymers, the cations from the interlayers of the pristine-layered silicates are exchanged with organic cations such as an alkylammonium, so the layered silicate attains a hydrophobic/organophilic character, which typically results in large interlayer spacing.[7] This increases the space between them and provides exfoliation of the layers and the intercalation of polymer chains between them. Montmorillonite is among the most commonly used smectite-type layered silicates for the preparation of nanocomposites.[8] The smectite clays are endowed with unique swelling, intercalation, and ion-exchange properties, stemmed from their layered structure, interlayer space (galleries), and residual load ($E+ = 0.33$).[9,10] Montmorillonite is a crystalline 2 : 1 layered clay mineral made of two sheets of silicon tetrahedrons and an intermediate sheet of aluminum octahedrons. Montmorillonite clay naturally forms stacks of plate-like structures, or platelets. The spaces between these platelets are called gallery spaces. The montmorillonite surface modification is used to match the polarity between the polymer matrix and the montmorillonite surface, but it also expands the clays' galleries. This facilitates the penetration of the gallery space by either the polymer precursors or the preformed polymer. Nanocomposites have been formed by various techniques such as *in situ* polymerization or melt-compounding.[11] In the *in situ* polymerization, clay is dispersed in the monomer, which is then polymerized. In the melt-compounding, the clay is mixed

Correspondence to: C. G. Salazar (cguerrer@ccr.dsi.uanl.mx).

© 2008 Wiley Periodicals, Inc.
WILEY InterScience® DISCOVER SOMETHING GREAT

with the preformed polymer in the molten state, where polymer chains diffuse into the space between the clay layers or galleries.[12,13] This technique decreases the time to form these hybrids by breaking up clay particles and increasing sample uniformity.[14] This promising approach would allow nanocomposites to be formulated directly using ordinary compounding devices such as extrusion or other mixers according to what is needed, without the necessary involvement of resin producers. The degree dispersion is governed by the matrix viscosity, average shear rate, and the mean residence time in the mixing process.[15] The scope of this work is the chemical montmorillonite surface modification, with the object of matching with the polymer matrix, to obtain nylon 6 nanocomposites by melt-compounding. We also study the necessary processing parameters to exfoliate the organoclay in the polymer matrix, using a twin-screw extruder. Mixtures were made with natural and modified montmorillonite obtaining nylon 6-organoclay nanocomposites. In addition, a Brabender Plasticorder was used for comparative purposes. All the cases used different percentages of clay content.

EXPERIMENTAL

Materials and preparation of nanocomposites

In this study, we used purified sodium montmorillonite (Kunipia F) supplied by Kunimine Industries (Tokyo, Japan). The cation exchange capacity (CEC) of unmodified montmorillonite-Na is 115 meq/100 g, with a specific surface area of 20.87 m^2/g. The montmorillonite was modified by trimethyl(tetradecyl) ammonium bromide (TTAB) of Sigma-Aldrich, and the nylon 6 used in this study is from BASF Plastic Materials with a M_n = 34,313 g/mol. Prior to each processing step, all materials containing nylon 6 were dried in a vacuum oven for at least 12 h at 80°C to avoid moisture-induced degradation reactions. Natural and modified montmorillonite were freeze-dried and stored in a desiccator until ready for use. Organoclays were prepared by replacing exchangeable metal cations of the clay layers with the alkylammonium cations, following the procedure described by Asongu.[16] First, the sodium natural montmorillonite (labeled as MNa) was prepared by replacing the Na^+ cations of the clay layers with Ca^{2+} cations, with the purpose of facilitating the introduction of alkylammonium cations. The recovered Ca-montmorillonite (labeled as MCa) was freeze-dried for at least 24 h. For the exchange with the alkylammonium, portions (100 g each) of the MCa were equilibrated with the alkylammonium salt (ALAS) for 24 h at room temperature. The ALAS was added in concentration of fivefold in excess of the CEC of the MCa. At the end of the exchange period, the organoclay was separated by centrifugation and washed with distilled water. Then it was freeze-dried, and the dried organoclays were stored in a desiccator until ready for use. Composites were prepared by melt-compounding using a Werner and Pfleiderer Type ZSK-30 twin-screw extruder. The compounding was carried out using a barrel temperature of 235°C, screw speed of 150 rpm, a feed rate of 1200 g/h, and the mean value of residence time at this condition was 3.2 min. Mixtures were made with natural and modified montmorillonite. For comparative purposes, a Brabender Plasticorder Type 6 with standard rotors and 60 cm^3 mixing head was used. The composites were mixed at 230°C at 100 rpm, under a nitrogen atmosphere. The polymer was melted first, until it reached its melting temperature (T_m). When the polymer achieved its T_m, montmorillonite was added. During 4 min both components were mixed. More details in Table I.

X-ray diffraction

XRD patterns were obtained to determine the mean interlayer spacing of the (001) plane ($d001$) for the natural and modified clay and the dispersibility of the silicate layers of montmorillonite in the composites. The XRD measurements were performed using a Siemens D-5000 instrument with Cu Kα radiation at scan rate of 0.05 2θ/min and 40 kV/30 mA. XRD measurements were made directly from MNa and MOrg in powder form. The nylon 6/MOrg (N6/MOrg) measurements were carried out in films, with different clay loads.

Nitrogen adsorption analyses

Nitrogen adsorption–desorption isotherms were measured at 77 K over a wide relative pressure range, using a Quantacrom, Autosorb-1 system. Samples of natural clay and organoclays were degassed

TABLE I
Composites Mixing Conditions

Device	Clay type	Composite name	Temperature	Residence time	Screw speed	Atmosphere	% Load
Twin-screw extruder	Organoclay	E-NYORG	235°C	3.2 min	250 rpm	Air	1%, 3%, 5%
	Natural	E-NYNAT	235°C	3.2 min	250 rpm	Air	1%, 3%, 5%
Brabender	Organoclay	B-NYORG	230°C	4 min	100 rpm	Nitrogen	1%, 3%, 5%

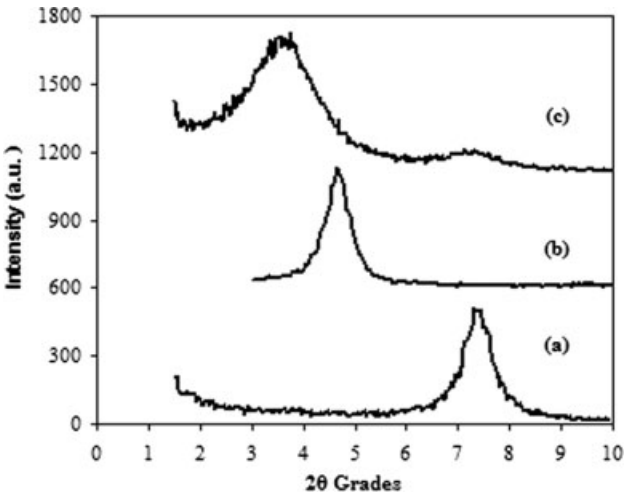

Figure 1 X-ray diffraction patterns of sodium natural montmorillonite, MNa (a); organic modified montmorillonite, MOrg (b); and Cloisite 20A, C20A (c).

under a vacuum of 10^{-3} Torr for 4 h at 423 K prior to the adsorption experiments. Specific surface areas were measured using the BET method. Pore diameter and pore size distribution were determined by the BJH method and the existence of microporosity tested from *t*-plot constructions.[17]

Fourier transform infrared spectroscopy

Infrared (IR) spectra were taken with a Fourier transform infrared (FTIR) spectrometer with a Perkin–Elmer model Spectrum GX. FTIR spectra were recorded between 4000 and 600 cm^{-1} by coadding 10 scans (background and sample) at a resolution of 3 cm^{-1}. FTIR spectra were obtained for the ALAS, nylon 6, and the composites at room temperature. Samples were analyzed as thin films.

Thermal properties

The thermal properties of nylon 6 and the various composites were determined by thermogravimetric analysis (TGA). The TGA was obtained with a TGA-50 Shimadzu. For the clays, TGAs were carried out under an air atmosphere, using a heating rate of 3°/min, from room temperature to 1000°C. The composites TGA analyses were carried out under an argon atmosphere, using a heating rate of 10°/min, from room temperature to 500°C.

Rheology properties

For rheological characterization, the fluid index for the composites and the nylon 6 was determined, according to ASTM D 1238. An Instron capillary rheometer was used to determine the logarithm viscosity versus shear rate graph at 235°C temperature.

Mechanical properties

Tensile testing was done using an Instron model machine at room temperature according to ASTM D 256. The specimens were prepared in filament form for the test. Modulus and yield strength were measured using a crosshead speed of 30 mm/min.

RESULTS AND DISCUSSION

Montmorillonite modification

Montmorillonite X-ray diffraction

XRD was used to determine the basal spacing of the MNa and the MOrg. The range of 2θ scanning of X-ray intensity employed was 1.5°–30°. For comparison purposes, a commercially modified montmorillonite Cloisite 20A supplied by Southern Clays products was used. The Cloisite 20A (labeled as C20A) is a natural montmorillonite modified with a quaternary ammonium salt. Figure 1 shows X-ray powder diffraction patterns for the MNa, MOrg, and C20A montmorillonites, respectively. The increment in the basal spacing measurement will confirm the presence of ALAS into the modified clay galleries. The pattern for MOrg exhibits a diffraction peak at 2θ = 4.65, leading to a basal spacing of $d(001)$ = 18.98 E. As a comparison, the pattern for the MNa showed a peak at 2θ = 7.44, leading to a basal spacing of $d(001)$ = 11.96 E. This demonstrates the layer expansion in the montmorillonite was modified by us. This effect was due to the intercalation of ion-exchanged ALAS among the clay layers. And the pattern of the C20A shows a higher layer expansion than the MOrg. Table II shows the basal spacing values to MNa, MOrg, and C20A.

Nitrogen adsorption analyses

Table III shows the pore structural characteristics of the different montmorillonite samples. The specific

TABLE II
Basal Spacing Measurement of the Clays

Name	Organic modifier	Basal spacing *d* (Å)
Na-montmorillonite MNa		11.96
Organoclay MOrg	Trymethyl (tetra-decyl) ammonium bromide	18.98
Cloisite 20A (C20A)	Dimethyl, dihydrogenatedtallow, quaternary ammonium	23.54

TABLE III
Pore Structure of Natural and Modified Montmorillonite Samples

	MNa	MOrg	C20A
BET area (m^2/g)	14.39	3.62	10.88
BJH method desorption pore diameter (Å)	38.04	35.33	35.99
t-Method micro pore surface area (m^2/g)	2.24	0.00	

surface area was calculated using the standard BET equation at *P*/*Po* (where *P* and *Po* denote the equilibrium and saturation pressures of nitrogen, respectively) which was between 0.06 and 0.2.

Figure 2 presents the pore size distribution applying the BJH model for the desorption isotherm. For MNa, the pore diameter of 38.04 Å presents a high and very remarkable value of volume, for MOrg and C20A the distribution is broader. Figure 3 compares isotherms of adsorption–desorption of N_2 at 77 K for both montomorillonites, MOrg and C20A, and in a separated plot the natural sodium montmorillonite MNa. Filled symbols indicates values of adsorption, open symbols indicate the desorption curve. The shapes of isotherms for both montomorillonites modified by us (MOrg) and the commercial (C20A), according to IUPAC classification, correspond to type V.[18] Isotherms indicate mesoporous material (2–50 nm of porous diameter) and showed flat adsorption and desorption branch under 0.4 of relative pressure (*P/Po*), that demonstrates weak adsorbate–adsorbent interactions. The hysteresis loop is type H3 for both organoclays; this type is usually given by aggregates of plately particles or adsorbents containing slit pores.[18,19] Both samples present very closed hysteresis loops, but C20A hysteresis loop approaches *P/Po* = 1, suggesting the presence of macropores (>50 nm). Natural montomorillonite (MNa) showed an IUPAC isotherm type IV that presents a hysteresis loop, which is usually associ-

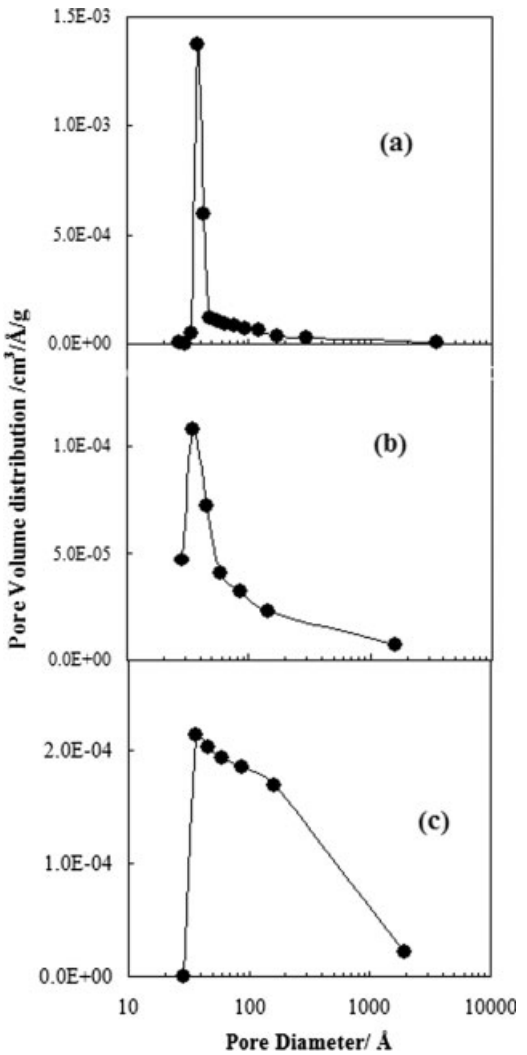

Figure 2 Pore size distribution of montmorillonite clays; natural MNa (a), modified MOrg (b), commercial Cloisite 20A, C20A (c).

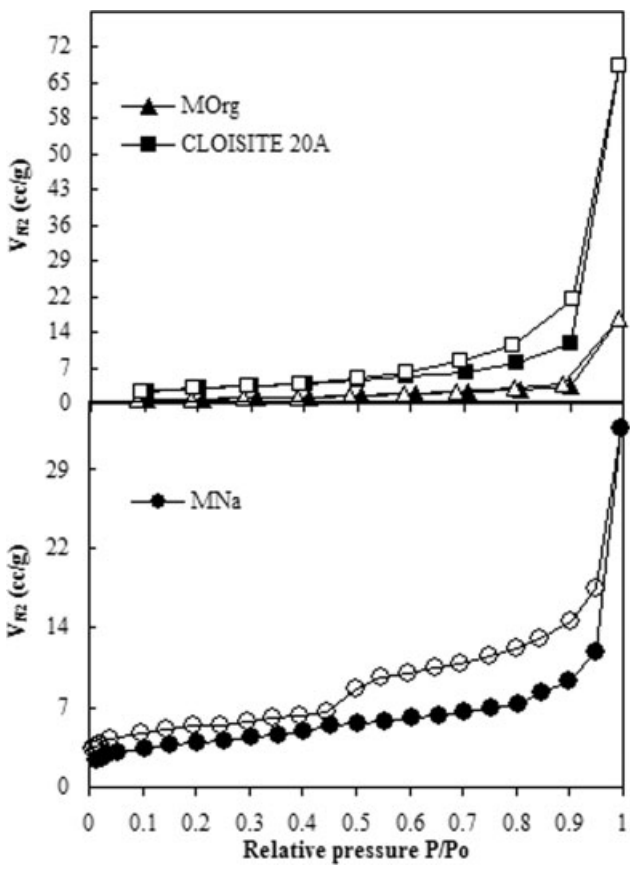

Figure 3 Liquid nitrogen sorption isotherms for modified montomorillonite (MOrg), commercial modified montmorillonite (CLOISITE 20A), and sodium natural montmorillonite (MNa).

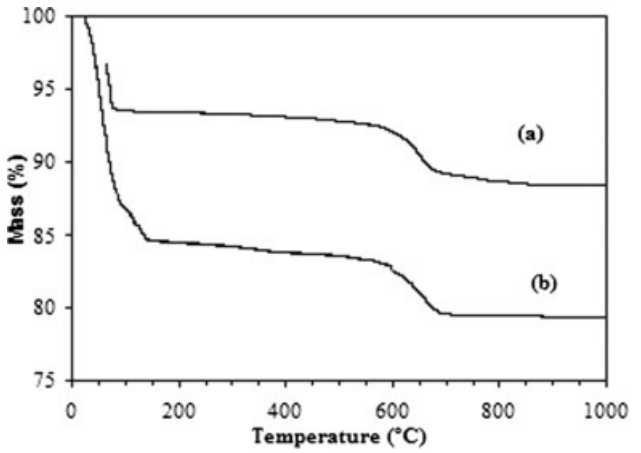

Figure 4 TGA curves for montmotillonite clays, heating velocity 3°C/min, air atmosphere. Sodium natural montmorillonite, MNa, curve (a), calcium montmorillonite, MCa, curve (b).

ated with filling and emptying of mesopores by capillary condensation.

A knee at low-relative pressures indicates the presence of micropores, which Table III confirms with the value of the surface area by *t*-method.[17] H3 type of hysteresis indicates a laminated material.[20] These results indicate that interchanged ALAS occupied the micropores. Mesoporous cavities remained after ALAS was interchanged, but hysteresis and knee absences in the isotherms of modified clay (MOrg) indicates that micropores or interconnection between mesoporous cavities could be occupied for the amide.

Thermogravimetric analysis

Figure 4 shows the TGA results for the MNa and MCa clays. The curve for MNa [curve labeled as (a)] shows the water content in the surface, this means the swelling capacity of the MNa. The MNa has 6.45% of free water content in its surface. To promote the intercalation of the ALAS in the montmorillonite layers surface, it was started with an exchange in the interlayer of Na cations for Ca cations, this promoted an increment to the montmorillonite layers basal spacing. Curve (b) shows the TGA results for the MCa. The MCa showed 15% of free water content on its surface. Figure 5 shows the amount of organic material that was measured in the MOrg. The mass of organic species that it contained was $\sim$ 28%. In curve (b) of Figure 5, two changes were observed which correspond to the weight loss of clay. The first change corresponds to the free water boiling, and the second one, which occurs between 400 and 800°C, is due to the recombination of the hydroxyl groups union or the boiling water united to these groups.[21] In the loss mass derivative curve, we can observe that the modifier ion did not degrade in only one temperature. In Figure 5, three different peaks were observed, where the modifier ion was degraded. The first occurred at 240°C because of the ALAS mixing effect of desorption of chemical bonded water and the first degradation step of the ALAS. The second and third peaks were referred to the total degradation (combustion).

Nanocomposites

MOrg/N6 nanocomposites X-ray diffraction

Figure 6 shows the XRD patterns. The pattern of the organoclay powder (MOrg) is labeled (a). The patterns of the composites of nylon 6 formed in the Brabender Plasticorder (B-NYORG) are labeled (b), (c) and (d); and the patterns of the composites formed in the twin-screw extruder (E-NYORG) are labeled (e), (f), and (g) with different MOrg load compositions in both composites.

The dispersion of fillers in a matrix is typically described in terms of exfoliation or intercalation.[22] Qualitative assessments made to evaluate the degree of clay dispersion are determined by XRD. Wu et al. have reported that the absence of the characteristic clay *d*(001) peak indicates the exfoliation of the clay platelets in the nylon 1012 matrix.[23] Similar results were also reported by Cho and Paul,[15] Jiang et al.,[24] and Douwe et al.[25] Composites with 1% MOrg load [patterns (B) and (E) in Figure 7] do not show any peak in the XRD pattern. This could be a hint that only a small portion of organoclay was exfoliated, or to the fact that the organoclay content is very small. This can be an indicator that the quantity is too small to be analyzed by the diffraction instrument used. For the B-NYORG, full exfoliation was not achieved, composites with 3% [curve (c)] and 5% of

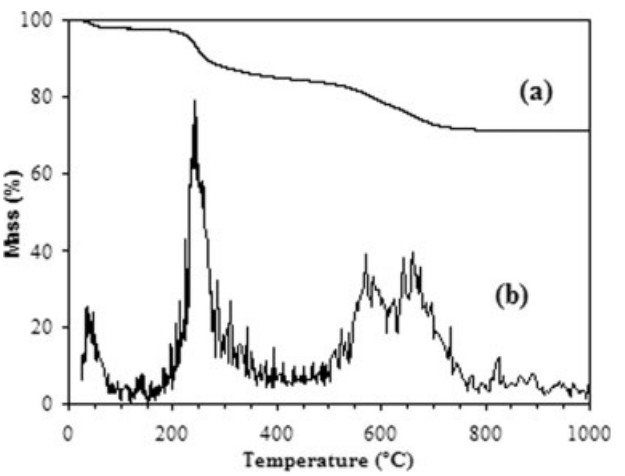

Figure 5 TGA curves for MNa (a) and MCa (b), heating velocity 3°C/min, air atmosphere.

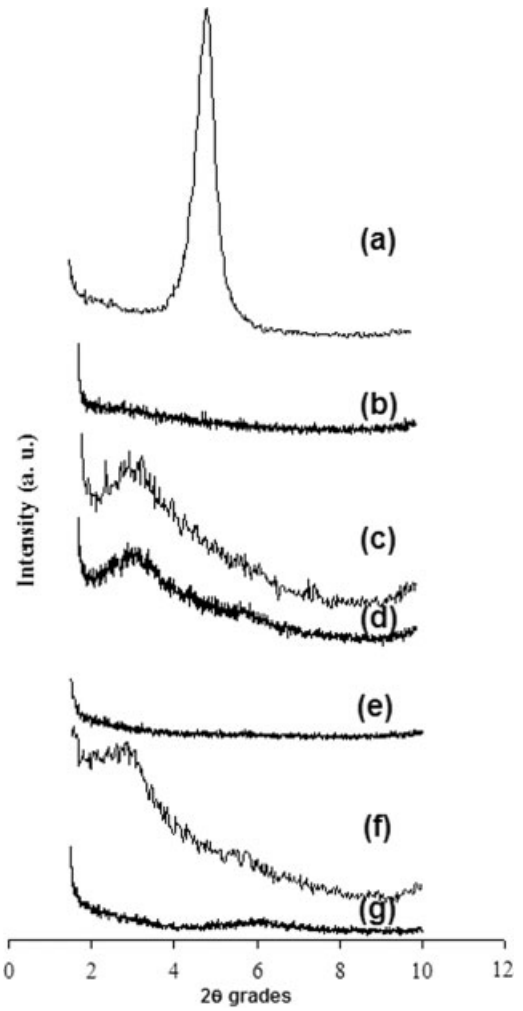

Figure 6 X-ray diffraction patterns for (a) MOrg powder, B-NYORG with (b) 1%, (c) 3%, and (d) 5% of MOrg load, and E-NYORG with (e) 1%, (f) 3%, and (g) 5% of MOrg load.

MOrg load [curve (d)] still show a peak at $2\theta = 3.02$ and 2.956, respectively, with a basal spacing of 29.23 E and 29.86 Å. This could mean that the Brabender Plasticorder is not an adequate system for our purposes; processing conditions are not suitable to get the layers exfoliation into the polymer matrix. E-NYORG prepared with 3% of MOrg load [curve (d)], exhibits one broad diffraction peak with basal spacing of 30.75 Å, corresponding to the layer separation of organoclay in the matrix, without getting full dispersion. On the other hand, composites with 5% MOrg load, Figure 6(g) reveals the formation of a dispersed nanocomposite, since the diffraction pattern does not show the characteristic clay *d*(001) diffraction peak. Although XRD patterns may not be regarded as being the most sensitive measure for describing the degree of intercalation or exfoliation of organoclay aggregates in a polymer matrix, they certainly are very useful to make qualitative observations.[7]

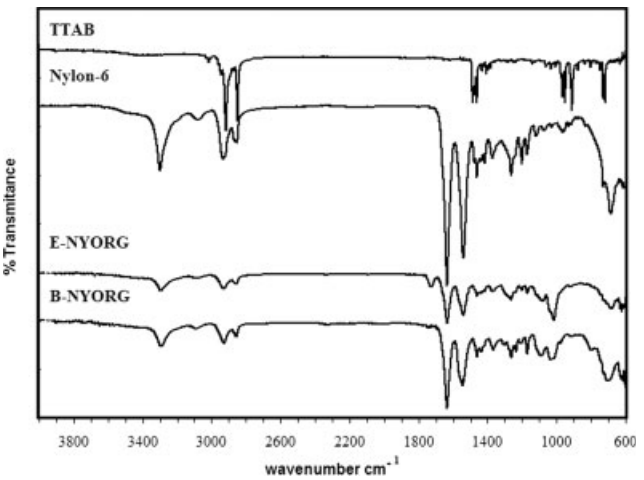

Figure 7 FTIR spectra for trymethyl(tetradecyl) ammonium bromide (TTAB), nylon 6, and composites processed by twin-screw extruder (E-NYORG) and Branbender Plasticorder (B-NYORG) both at 5 wt % of organoclay.

Fourier transform infrared spectroscopy

Table IV lists the position of bands in IR spectra of the TTAB, nylon 6, and the composites E-NYORG and B-NYORG, and some bands are identified in the assignment column. Figure 7 presents the FTIR spectra of TTAB and nylon 6. The typical strong bands for the polyamide 6 are at 3300 cm^{-1} (hydrogen bonded *N*—H stretch), 1640 cm^{-1} (Amide I, C=O stretch), and 1545 cm^{-1} (Amide II, C—N stretch + C(O)—*N*—H bend) of wavenumber.[26] In the spectrum for TTAB, it was observed at 3300 cm^{-1}, does not show the peak of the *N*—H bond. The absence of this bond corroborates that the ammonium salt is a tertiary one. The characteristic bands for the aluminosilicate structures can usually be observed between 1200 and 400 cm^{-1}, among which the most intense is situated in the 1040–990 cm^{-1} region, due to Si—O stretching vibrations.[3] Figure 8 shows the FTIR spectra for the E-NYNAT, E-NYORG, and B-NYORG composites in the region containing the peak of the Si—O stretching vibration at about 1015 cm^{-1}. This demonstrates the addition of the clay at the polyamide matrix. In the E-NYNAT spectra the peak of the Si—O stretching vibration is very sharp, and the position of the band for E-NYNAT with different load clay is the same at 1015 cm^{-1}. In the spectrum for the E-NYORG and the B-NYORG composites, the peaks were broader and deformed with the addition of the organoclay, in both cases, due to the intercalation of the ALAS between the clay layers. The IR absorption technique was used to identify the interactions between the TTAB and NYLON 6 in the composites. The chemical interaction between functional groups of the polymer and the surface-modified organo-silicate layers improves the penetration of the polymer into the interlayer

TABLE IV
Position of Bands in Infrared Spectra

TTAB	Nylon 6	E-NYNAT 5%	E-NYORG 5%	B-NYORG 5%	Assignment
–	3296.5 (m)	3286 (m)	3294 (w)	3288 (w)	N—H stretch
–	3082 (vw)	3094 (w)	3073.5 (vw)	3084.5 (vw)	
3015 (vw)	–	–	–	–	
–	2930 (m)	2926.5 (m)	2928 (w)	2924 (w)	
2915.5 (m)	–	–	–	–	
2848.5 (m)	2853.5 (w)	2854.5 (w)	2854 (w)	2854 (w)	
		1723 (w)	1722.5 (w)		
–	1634 (vs)	1633 (vs)	1632.5 (m)	1633.5 (s)	Amide I, C=O stretch
–	1538.5 (vs)	1544 (s)	1539.5 (m)	1543 (m)	Amide II, C—N stretch + C(O)—N—H bend
1487 (m)	–	–	–	–	
1462.5 (m)	1462 (w)	1461.5 (m)	1460.5 (w)	1460 (w)	CH_2 bend
1431.5 (m)	1437.5 (vw)	1437.5 (w)	1437 (vw)	1436 (vw)	CH_2 bend
–	1416 (w)	–	1418 (vw)	–	CO-vic CH_2 bend (α)
1407.5 (w)	–	–	–	–	
1395.5 (w)	–	–	–	–	
1382 (w)	–	–	–	–	CH_3 (trimethyl)
–	1369.5 (w)	1366.5 (w)	1370 (w)	1364.5 (w)	
–	1261 (w)	1263.5 (w)	1262.5 (w)	1261 (w)	Amide III
–	–	1234 (vw)	–	–	
–	–	1213.5 (vw)	–	–	
–	1200 (w)	–	1201.5 (vw)	–	(α)
–	1168 (w)	1169 (m)	1168.5 (vw)	1169 (w)	(γ, am.)
1140.5 (w)	–	–	–	–	
–	1120.5 (vw)	1119.5 (vw)	–	–	(am.)
–	–	–	–	1090.5 (w)	Si—O stretch
–	1074 (vw)	1075 (vw)	–	–	CONH, Si—O stretch
1062 (w)	–	–	–	–	
1032.5 (w)	1029 (vw)	–	–	1031 (w)	CONH, Si—O stretch
–	–	1016 (w)	1015 (m)	–	Si—O stretch
964.5	962	974 (vw)	–	973	C—CO stretch (α or γ)
950.5 (m)	–	–	–	–	
–	928.5 (vw)	–	–	–	C—CO stretch (α or γ)
911 (m)	–	–	–	–	
	834 (vw)	–	–	–	
730 (m)	728.5 (vw)	727 (vw)	–	–	CH_2 wag
719 (m)	–	–	–	–	
–	–	708 (w)	–	706 (m)	
–	685 (m)	–	680 (w)	–	Amide V (α)
–	618 (vw)	620 (vw)	621 (vw)	–	

space of the modified clay, being responsible for the changes observed in the IR signature of the polymer.[3]

The FTIR spectra of E-NYORG and B-NYORG composites at 5% of organoclay load are presented in Figure 7. The peaks, which represent the methyl groups, can be observed located in the region at almost 3000 cm^{-1}.[27] The peaks of the ALAS in this zone most probably overlapped the methyl groups of the nylon 6. Nylon 6 has been thoroughly studied in the past and it is well-known that it is able to crystallize in at least two crystalline structures, α and γ.[28] The presence of γ-crystals in nylon 6 is evidenced by the dominant peaks at 1122 and 976 cm^{-1}. The presence of a weak shoulder at 929 cm^{-1} and a strong amide II vibration at 1548 cm^{-1} indicate that there are also some α-crystals present in the nanocomposite.[29] In nylon 6 were observed γ and α crystal phases. This is defined as a strong and sharp peak at 1538 cm^{-1} for the α-phase (Fig. 7), and there are two very weak peaks for the γ-phase, at a very low frequency of 1120 and 962 cm^{-1} (Fig. 8).

Medellín-RodrÙíguez et al. postulated that on linear heating, the unstable γ-structure is able to recrystallize to the most stable α-form and crystals followed by a step-like melting mechanism.[30] In the composites the γ-crystal evidence was kept only in the E-NYNAT composites, in which the clay load content did not affect the γ-phase (Fig. 8). In the E-NYORG composites the γ-peaks seem to be lightly present, only at 3% of organoclay load, a little peak was present at 972 cm^{-1}, and the other peaks, in all organoclay content appeared broader than the net nylon 6 (Fig. 8). The B-NYORG composites, kept the γ-phase at 1% of organoclay load, but at 3 and 5% of

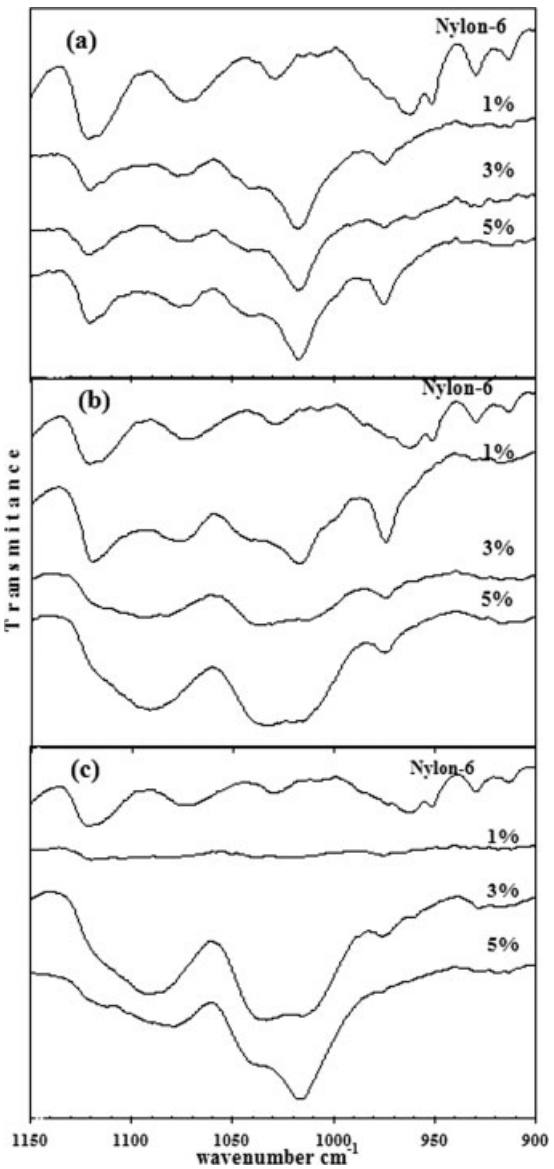

Figure 8 FTIR of composites in the range of 1150–900 cm^{-1}; E-NYNAT at different natural sodium montmorollonite loads (a), B-NYORG (b) and E-NYORG (c) both at different organoclay loads. Nylon 6 spectra showed for comparison.

organoclay load these peaks were broader and deformed (Fig. 8). The α-phase was present in all the composites, between 1539.5 and 1544 cm^{-1}, with strong and medium bands. It has been postulated that the clay particles facilitate preferential formation of the γ-crystals near the clay surface.[31]

Thermal properties

The thermal stability of composites was studied to see the effect of load clay in the nylon composites by TGA. Figure 9 shows the weight loss because of the formation of volatile products after degradation at high temperature, as a function of temperature for the nylon 6 and the composites. It is reported that some nanocomposites combined with montmorillonite and polymer matrix can improve thermal stability.[32,33] The increase of thermal stability is attributed to the hindered diffusion of volatile decomposition products within the nanocomposites.[34] The majority of the composites have a higher decomposition temperature than the pristine nylon 6, only the E-NYNAT composite with 3% of load clay has a lower decomposition temperature than nylon 6. Table V shows the decomposition temperature for all the composites. The B-NYORG composites with 3 and 5% of load clay have the highest decomposition temperature. Both have similar decomposition temperatures, 445.519°C (3%) and 445.072°C (5%).

In the E-NYORG composites the addition of clay does not show a relevant change over decomposition temperature, at 3% of load clay the temperature was kept similar to the pristine nylon 6, and at 5% of

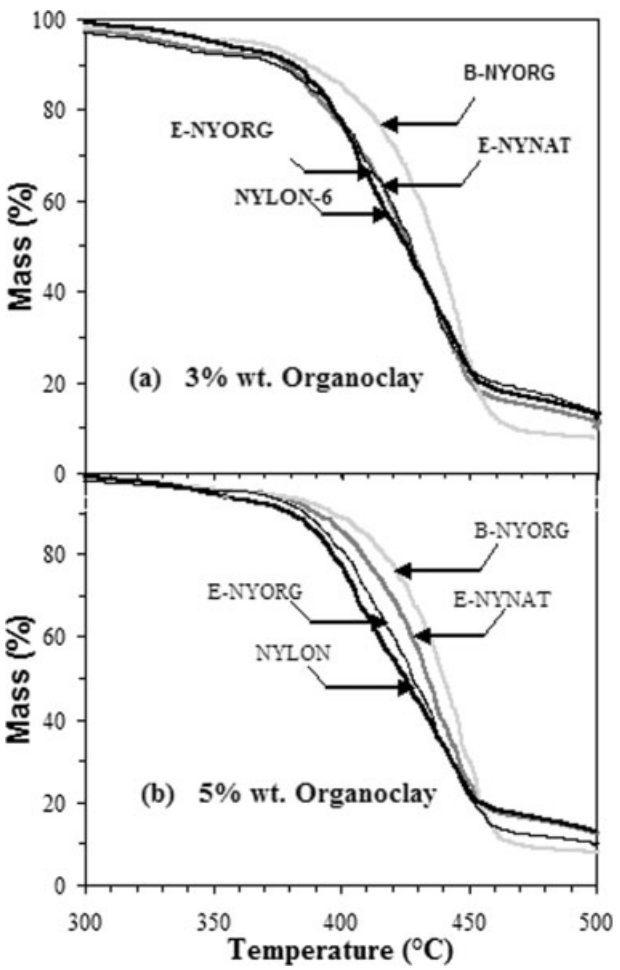

Figure 9 TGA curves of the composites at 3 wt % (a) and 5 wt % (b) of organoclay load, compared with the nylon 6. Heating rate 3°C/min in atmosphere of argon.

TABLE V
Decomposition Temperature for the Nylon 6 and the Composites

Polyamide composites	MOrg content	Decomposition temperature (°C)
Nylon-6	0%	433.87
	3%	432.84
E-NYNAT	3%	432.84
	5%	439.585
E-NYORG	3%	433.269
	5%	435.274
B-NYORG	3%	445.519
	5%	445.072

load clay the temperature only has a 2°C increment. The composites made with natural montmorillonite (E-NYNAT) only had an increment over the decomposition temperature at 5% of load clay at 439.585°C.

Rheology

The melt-flow index (MFI) for the composites was obtained according to ASTM D 1238. Analyses were carried out at 235°C with 2060 g of load. The results are shown in Figure 10. The MOrg content in the composites may affect the rheological properties in the melted state. In the E-NYORG, the MFI diminished with the addition of organoclay in the polymer matrix, increasing the viscosity. Meanwhile in the E-NYNAT composites, the MFI was kept constant in all the compositions. Rheological properties of nanocomposites formed from MOrg were analyzed; we obtained the shear viscosity behavior of net nylon 6 and various composites at low shear rates measured by capillary rheometry according to ASTM D 3835 (Fig. 11). The diameter of the capillary used was 1.0005 mm and height of 30.03 mm, analysis was carried out at 235°C. The composites formed from MOrg (E-NYORG) exhibited similar shear thinning behavior as net nylon, because of the lower load of organoclay and the shear rate used. The composites

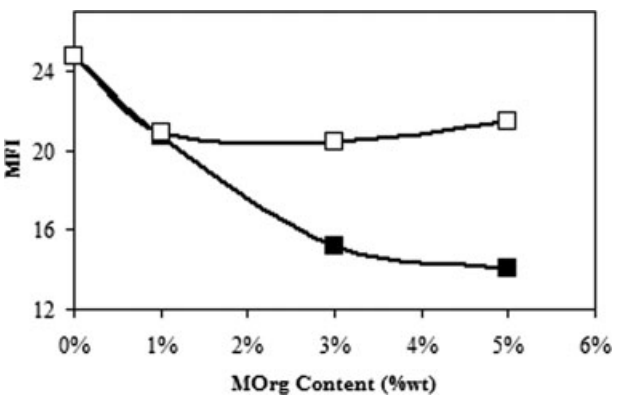

Figure 10 Melt-flow index (MFI) as a function of %MOrg content for E-NYORG (filled) and E-NYNAT (not filled).

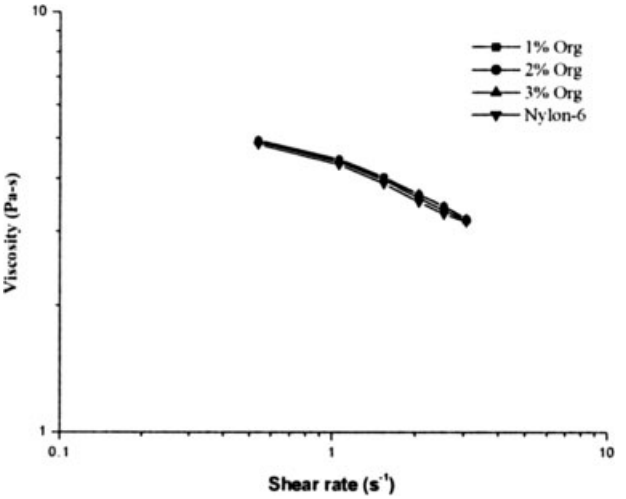

Figure 11 Melt viscosity as a function of shear rate for the net nylon 6 and the E-NYORG at 235°C.

made with natural montmorillonite show a little difference with the net nylon (Fig. 12), the viscosity for the composites with 1 and 3% of natural montmorillonite load was higher than the pristine nylon 6, which implies a worse dispersion of the clay layers in the polymer matrix.

Mechanical properties

A summary of the mechanical properties of composites prepared in the twin-screw extruder with natural and modified clay are shown in Table VI. The values indicate that the clay content has a significant effect on the mechanical properties, in spite of the low clay content. Figure 13 shows the effect of inorganic filler content (wt % MOrg) on composite modules, yield point, and elongation at break.

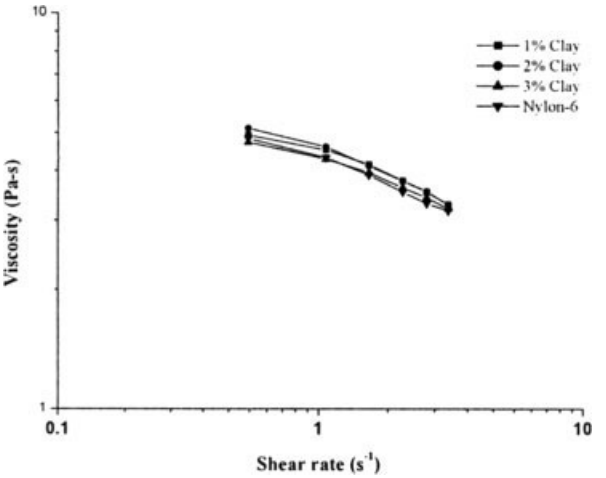

Figure 12 Melt viscosity as a function of shear rate for the net nylon 6 and the E-NYNAT at 235°C.

TABLE VI
A Summary of the Mechanical Properties of Composites Prepared in the Twin-Screw Extruder with Natural and Modified

Polyamide composites	MOrg content	Tensile Modulus (GPa)	Yield Point (YP) (MPa)	Elongation at break (%)
Nylon 6	*0*	*1.986*	*60.881*	22.672
E-NYORG	*1%*	*2.833*	*67.500*	3.497
	3%	*3.097*	*62.587*	2.413
	5%	*3.122*	*53.365*	1.640
E-NYNAT	*1%*	2.051	16.644	4.832
	3%	2.049	14.532	3.240
	5%	2.041	14.215	4.202

For the E-NYORG composites the tensile modulus has a progressive increment as function of the MOrg load [Fig. 13(a)]. Filled symbols indicate values for E-NYORG and open symbols indicate values for E-NYAT samples, respectively. The tensile modulus for the E-NYORG with 5% of organoclay content increased 57% compared with the net nylon [see Fig. 13(a)]. The E-NYNAT composites do not show a relevant change in respect to the increase of the clay content in the matrix.

On the other hand, the yield strength in the E-NYORG composites does not show a clear dependency on the MOrg content. At 1% of organoclay content the composite has a poor improvement with respect to the net nylon 6, and for the compositions with 3 and 5% of organoclay content, the yield strength declined with the addition of organoclay. In the E-NYNAT composites the yield strength was dramatically decreased with the addition of the clay, the yield strength behavior was almost constant for the different load compositions [Fig. 13(b)].

The ductility of the composites, as determined by elongation at break, upon increasing the clay concentration results in an equivalent sacrifice in ductility at the 30 mm/min testing speed [Fig. 13(c)]. Both composites, the E-NYORG and the E-NYNAT, have a similar behavior with the addition of clay in all their compositions. The ductility was greatly affected, even with a small content of clay (1%). After the addition of organoclay the behavior it was maintaining was very similar.

This mechanical testing shows us that the increment of natural montmorillonite content in the nylon 6 matrix does not improve or worsen the characteristics of the composites. These characteristics were more or less the same with different load clays. Interestingly, the composites made with organoclay have a very different behavior in these mechanical tests, the modulus was substantially increased in relation to the net nylon 6.

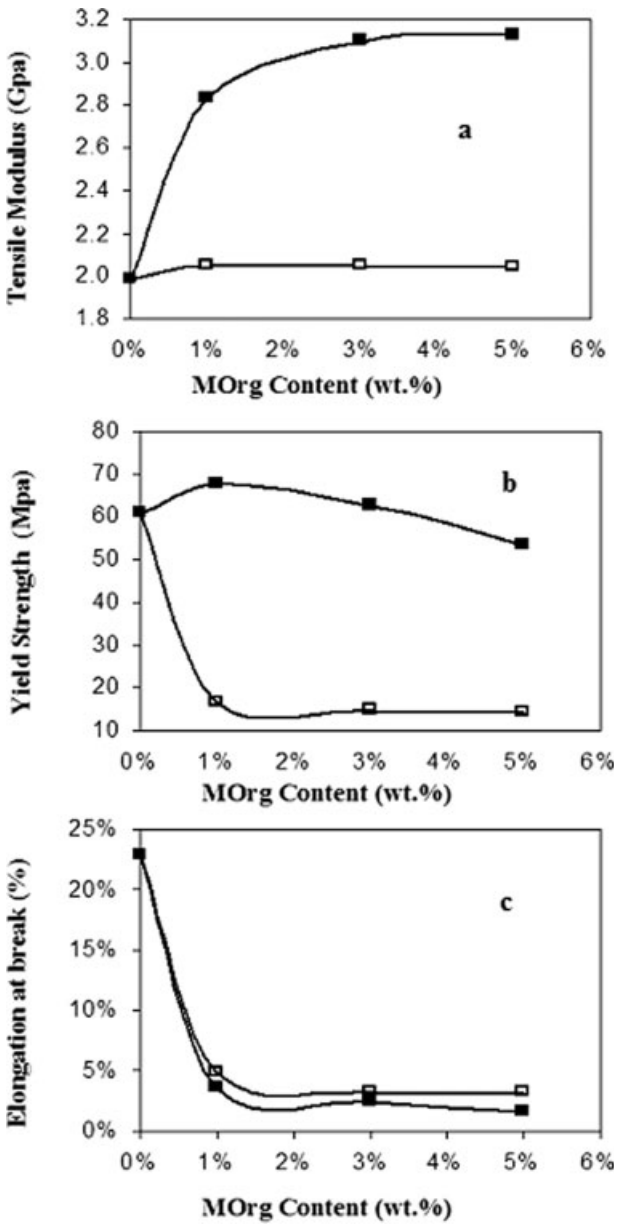

Figure 13 (a) Tension modulus (b) yield point, and (c) elongation at break for E-NYORG as a function of MOrg content.

CONCLUSIONS

The result obtained from the chemical surface modification of the montmorillonite clay with TTAB was

satisfactory. The basal spacing obtained in the oganoclay was 18.98 Å.

In the TGA results for the clays, we can appreciate the degradation temperature of the ALAS in the organoclay that starts from 180°C, having the maximum degradation rate at 240°C. This temperature implies the election of the polymer matrix that we can use for the processing. The composites made with nylon 6 with 5% of organoclay of load that were processed in a twin-screw extruder revealed the formation of a dispersed nanocomposite according to the results in XRD pattern. The use of a Brabender Plasticorder was less effective to obtain an exfoliation in the composites studied. The crystalline α-structure was more stable in all nylon composites than the crystalline γ-structure. On the other hand, the increment of the organoclay content in the E-NYORG composites improve the tension modulus, and the yield point was affected by this cause too.

References

1. Le Baron, P. C.; Wang, Z.; Pinnavia, T. Appl Clay Sci 1999, 15, 11.
2. Johnston, C. T.; Premachandra, G. S. Langmuir 2001, 17, 3712.
3. Viville, P.; Lazzaroni, R.; Mollet, E.; Alexandre, M.; Dubois, P.; Borcia, G. Langmuir 2003, 19, 9425.
4. Vaia, R. A.; Liu, W. J Polym Sci Part B: Polym Phys 2002, 40, 1590.
5. Sur, G. S.; Sun, H. L.; Lyu, S. G.; Mark, J. E. Polymer 2001, 42, 9783.
6. Hyun, Y. H.; Lim, S.; Choi, H. J.; Jhon, M. S. Macromolecules 2001, 34, 8084.
7. Lee, K. M.; Han, C. D. Macromolecules 2003, 36, 7165.
8. Ray, S. S.; Okamoto, M. Polym Sci 2003, 28, 1539.
9. Bourlinos, A. B.; Karakassides, M. A.; Simopoulos, A.; Petridis, D. Chem Mater 2000, 12, 2640.
10. Schifter Domínguez, J. M.; Schifter Dominguez, I. Las arcillas: el barro noble; Fondo de Cultura Económica: Mexico, 1995.
11. Yoon, P. J.; Fornes, T. D.; Paul, D. R. Polymer 2002, 43, 6727.
12. Solomon, M. J.; Almusallam, A. S.; Seefeldt, K. F. Macromolecules 2001, 34, 1864.
13. Guido, K. Polym Sci 2003, 28, 83.
14. Kim, S. W.; Jo, W. H.; Lee, M. S.; Ko, M. B.; Young, J. Polym J 2002, 34, 103.
15. Cho, J. W.; Paul, D. R. Polymer 2001, 42, 1083.
16. Asongu, V. Doc. Thesis, Georgia Institute of Technology, Atlanta, 1993.
17. Gregg, S. J.; Sing, K. S. W. Adsorption, Surface and Porosity, 2nd ed.; Academic Press: London, 1982.
18. Sing, K. S. W.; Everett, D. H.; Haul, R. A. W.; Moscou, L.; Pierotti, R. A.; Rouquérol, J.; Siemieniewska, T. Pure Appl Chem 1985, 57, 603.
19. Yu, H.; Yu, J.; Cheng, B.; Zhou, M. J Solid State Chem 2006, 179, 349.
20. Williams, P. T.; Reed, A. R. Biomass Bionergy 2006, 30, 144.
21. Le Pluart, L. D. C. Thesis, L'Institut National de Sciences Appliquées de Lyon, Lyon, 2002.
22. Weon, J.-I.; Sue, H.-J. Polymer 2005, 46, 6325.
23. Wu, Z.; Zhou, C.; Qi, R.; Zhang, H. J Appl Polym Sci 2002, 83, 2403.
24. Jiang, T.; Wang, Y.-H.; Yeh, J.-T.; Fan, Z.-Q. Eur Polym J 2005, 41, 459.
25. Homminga, D. S.; Goderis, B.; Mathot, V. B. F.; Groeninckx, G. Polymer 2006, 47, 1620.
26. Kohan, M. I. Nylon Plastics Handbook; Hanser: Munich, 1995.
27. Bruice, P. Y. Organic Chemistry, 3rd ed. Prentice Hall: Eaglewood Cliffs, NJ, 2001.
28. Loo, L. S.; Gleason, K. K. Macromolecules 2003, 36, 2587.
29. Zapata-Espinosa, A.; Medellín-RodrÙíguez, F. J.; Stribeck, N.; Almendarez-Camarillo, A.; Vega-Díaz, S.; Hsiao, B. S.; Chu, B. Macromolecules 2005, 38, 4246.
30. Medellín-RodrÙíguez, F. J.; Larios-López, L.; Zapata-Espinosa, A.; Phillips, P. J.; Dávalos-Montoya, O.; Lin, J. S. Macromolecules 2004, 37, 1799.
31. Lincoln, D. M.; Vaia, R. A.; Wang, Z.-G.; Hsiao, B. S. Polymer 2001, 42, 1621.
32. Burnside, S. D.; Giannelis, E. P. Chem Mater 1995, 7, 1597.
33. Lee, J.; Takekoshi, T.; Giannelis, E. P. Mater Res Soc Symp Proc 1997, 457, 513.
34. Gilman, J. W.; Jackson, C. L.; Morgan, A. B.; Harris, R.; Manias, E.; Gannelis, E. P.; Wuthenow, M.; Hilton, D.; Phillips, S. H. Chem Mater 2000, 12, 1866.